Original Research

Endoplasmic reticulum stress-mediated apoptosis in imatinib-resistant leukemic K562-r cells triggered by AMN107 combined with arsenic trioxide

Yuan Xia[1,2], Hai Fang[3], Ji Zhang[1,3] and Yanzhi Du[1]

[1]Key Laboratory of Stem Cell Biology, Institute of Health Sciences, Shanghai Institutes for Biological Sciences (SIBS), Chinese Academy of Sciences (CAS) and Shanghai Jiao Tong University School of Medicine (SJTU-SM), Shanghai 200025, China; [2]Graduate School of the Chinese Academy of Sciences, Beijing, 100049, China; [3]State Key Laboratory of Medical Genomics and Sino-French Research Center for Life Sciences and Genomics, Ruijin Hospital, SJTU-SM, Shanghai 200025, China
Corresponding author: Yanzhi Du. Email: yzdu@sibs.ac.cn

Abstract

The first tyrosine kinase inhibitor (TKI) imatinib mesylate (imatinib) targets the kinase domain of BCR-ABL and induces apoptosis in newly diagnosed chronic myeloid leukaemia (CML). However, resistant and relapse are common problems in imatinib-treated patients. Although second-generation TKI such as AMN107 appears to improve the treatment of CML, TKI resistance and relapse are also frequently occurred in the patients. To test whether arsenic trioxide (ATO) could potentiate the efficacy of AMN107 in imatinib-resistant cells, we conducted a series of assays in TKI-resistant K562-r cells treated with AMN107 and ATO. Based on a time-course cDNA microarray analysis, we found many genes typically involved in the endoplasmic reticulum (ER) stress signalling were significantly up-regulated, implicating the occurrence of ER stress-mediated apoptosis in K562-r cells treated with the combination of ATO and AMN107. Such implication was also supported by the data showing the activation of members in the JNK pathway, which are known to be characteristic markers bridging ER-stress and apoptosis. Partial knock-down of the JNK activities alleviated the effects of apoptosis ($p < 0.05$) triggered by combining AMN107 with ATO. In conclusion, this study for the first time demonstrates a synergistic effect of AMN107 with ATO, allowing insights into the possible mechanisms underlying imatinib-induced resistance in CML. Our data also suggest that combination of AMN107 with ATO may represent a new strategy for the treatment of imatinib-resistant CML patients.

Keywords: Chronic myeloid leukaemia, ER stress, apoptosis, imatinib-resistant cells, arsenic trioxide, AMN107

***Experimental Biology and Medicine* 2013; 238: 932–942. DOI: 10.1177/1535370213492689**

Introduction

Chronic myeloid leukaemia (CML) is a myeloproliferative disorder associated with a characteristic chromosomal translocation t(9;22) encoding the BCR-ABL fusion protein. This oncoprotein is the critical pathophysiological factor in the genesis and evolution of CML, and its existence is necessary and sufficient for the initiation and propagation of CML.[1,2] Imatinib mesylate (STI571, Gleevec) is the first tyrosine kinase inhibitor (TKI) targeting the kinase domain of BCR-ABL and effective for newly diagnosed chronic phase (CP)-CML.[3] The clinical application of imatinib has revolutionized the therapy of CML and has become the first-line treatment for the patients, yielding remarkable results with 83% of the event-free survival at six years and 93% of the rate of freedom from progression to accelerated phase (AP)/blast crisis (BC).[4–6] However, over one-third of the patients either fail to respond to imatinib and progress into blast phase/lack of tolerance.[7,8] Because the resistance to imatinib appeared at an unprecedented rate, a complete understanding of the pathways tied up with these escape mechanisms is required imminently.

Significant progresses have been made over the last decade in revealing the molecular mechanisms of imatinib resistance. The occurrence of resistance is BCR-ABL dependent or independent. On the one hand, *BCR-ABL* gene mutation or amplification can cause clinical resistance to imatinib,[9] in which many mutations are characterized through sequencing, including the P-loop, C-helix, SH2 domain, substrate-binding site, A-loop and C-terminal

lobe, and some of the mutations occurred even before the initiation of TKI-based therapies.[10] On the other hand, BCR-ABL independent mechanisms also play a part. Drug efflux and influx system, such as P-glycoprotein (Pgp) efflux pump and uptake transporters, especially the organic cation transporter (hOCT1), have also been proved as a potential source of imatinib resistance.[11–13] Other signalling pathways such as the Src family kinases have been implicated as a factor in altering responsiveness to TKIs, as well as mediating cellular transformation and promoting disease progression.[14–16]

To overcome imatinib resistance and to increase responsiveness of TKIs, new agents were developed. AMN107 (Tasigna, Nilotinib), while still targeting BCR-ABL, optimizing the potency and selectivity against BCR–ABL, is more effective than imatinib not only in patients with wild-type BCR-ABL but also with mutant forms.[17–21] It has been recently reported that there were fewer progressions to AP or BC in the AMN107 treatment groups, compared to the imatinib treatment group. Also, fewer CML-related deaths have been reported in the AMN107 groups, compared to the imatinib group. Overall, AMN107 shows better efficacy than imatinib for the treatment of patients with newly diagnosed CML in chronic phase without or with BCR-ABL mutations.[22] For CML patients acquiring BCR-ABL independent resistance and patients in blast phase, however, the effectiveness of AMN107 is still unsatisfactory, building an argument whether TKI of BCR-ABL alone can achieve satisfactory results.[19,23,24] Thus, the treatment of imatinib-resistant CML remains to be challenging and the strategy combining TKI with other anti-cancer agents is widely considered in CML therapy studies.[25,26]

Despite the well-known toxicity, arsenic trioxide (ATO) has been proven of biomedical beneficial, dating back to traditional Chinese medicine, and is now used worldwide to treat patients with APL who have undergone relapse from their primary therapy.[27,28] Therapeutic benefits of ATO include antiproliferation, antiangiogenesis, promotion of differentiation, and induction of apoptosis in a wide variety of malignancies.[29,30] We and others have previously shown that ATO and arsenic sulphide (As_4S_4) are effective in improving CML treatment effects.[31–34] ATO exerts its effect by affecting numerous intracellular functions, such as production of reactive oxygen species (ROS), modification of mitochondrial membrane potential, interfering with signalling pathways, alteration of gene regulation, and induction of DNA and protein damage.[35–37]

Due to the toxic nature of arsenic, ATO has limited clinical application as a single chemotherapeutic agent. However, it appears to be a promising therapeutic agent in combination with a variety of chemotherapeutic agents.[38–40] Herein, we investigated the therapeutic efficacy of AMN107 combined with ATO in the imatinib-resistant K562-r cells, which neither has *BCR–ABL* mutants nor overexpresses *BCR–ABL*. In this study, experiments were conducted to analyse the genes modulated over the time course through transcriptome analysis and to molecularly explore some of the key pathways underlying the combined therapy.

Materials and methods

Cell lines and reagents

The CML-derived cell line K562 from the American Type Culture Collection (Manassas, VA) and the imatinib-resistant K562-r[41] cell line, kindly provided by Dr. Melo JV, were cultured in RPMI 1640 (Gibco BRL, Life Technologies, Paisley, UK) supplemented with 10% v/v foetal bovine serum (PAA, Linz, Austria), 1% glutamine, and antibiotics (100 U/mL penicillin and 100 μg/mL streptomycin) in a 37°C incubator with a humidified atmosphere containing 5% CO_2. Imatinib and AMN107 were kindly provided by Novartis Pharmacy (Basel, Switzerland). Stock solutions (10 mM) were prepared in dimethyl sulphoxide (DMSO, Sigma, St Louis, MO) and stored in aliquots at −20°C. ATO and Vitamin C were purchased from Sigma (St Louis, MO) and dissolved in distilled water.

Cell growth and apoptosis assessments

K562-r cells were treated with 8 μM AMN107, 1.5 μM ATO, or the combination of the two for 24, 48 or 72 hrs in culture. Cell viability was measured by counting the cells, excluding those stained with 0.2% trypan blue. Exponentially growing cells were used and all experiments were performed in triplicates. MTT assay was used to estimate cell viability and proliferation.

Apoptosis assays were performed using Annexin V-FITC apoptosis detection kit (BD Biosciences PharMingen, San Diego, CA). Early apoptotic cells were stained positively with Annexin V only and late apoptotic cells were stained positively for both Annexin V and propidium iodide (PI). Mitochondrial transmembrane potential ($\Delta\Psi m$) was evaluated using rhodamine 123 (Sigma, St Louis, MO) plus PI staining. Cells stained positively for rhodamine 123 were considered losing mitochondrial transmembrane potential. All stained cells were followed with analysis of flow cytometry (FACSC500 flow cytometry; Becton Dickinson, San Diego, CA).

Gene expression profiling and data preprocessing

For gene expression profiling, time-course samples of K562-r cells were treated with 8 μM AMN107, 1.5 μM ATO, or the combination of the two, and then used for RNA extraction and microarray hybridization. Total RNA (30 μg) was used for microarray analysis. Array fabrication, reverse transcriptional labelling, and hybridization were performed as described previously.[42,33] The criteria for identifying the top significant transcripts were based on Benjamini and Hochberg-derived False discovery rate (FDR) <0.01. The expression matrix was subjected to the topology-preserving feature selection through the self-organizing map with singular value decomposition (SOM-SVD). The resulting data were then subjected to SOM-based two-phase gene clustering. Illustration of the SOM outputs by component plane presentations (CPPs) was conducted in the Matlab 6.5 environment as described previously.[42,43] Gene functional clustering was based on the online DAVID Bioinformatics Resources 6.7 (http://david.abcc.ncifcrf.gov) using diverse external annotated databases including Gene Ontology,[44]

and OMIM disorder-gene association information.[45] The transcriptome profiling is available at GEO accession GSE24946.

Detection of spliced XBP1 mRNA

Total RNA was used to perform reverse transcription–polymerase chain reaction, and detected both spliced and unspliced *XBP1* mRNA. Glucose-6-phosphate dehydrogenase (GAPDH) was used as a housekeeping gene control. Products were separated on 2% agarose gels. Size of PCR products: unspliced *XBP1* = 473 bp; spliced *XBP1* = 447 bp. The *XBP1* specific primers: sense, 5-AAACAGAG TAGCAGCTCAGACTGC-3; antisense, 5-TCCTTCTGG GTAGACCTCTGGGAG-3.

Quantitative real-time reverse transcription–polymerase chain reaction (RT-PCR)

RT-PCR was conducted for 10 randomly selected genes. Total RNA was isolated from K562-r cells using the RNeasy Mini kit (Qiagen, Valencia, CA), following the protocol suggested by the manufacturer. Then, RNA was reverse-transcribed employing High Capacity RNA-to-cDNA Kit (Applied Biosystems, CA). The cDNA were used as templates for real-time PCR performed in the 7900HT Fast Real-Time PCR System using SYBR Green I (Applied Biosystems, CA). The fold changes in expression of the different genes were compared with that of untreated control cells, normalized to the expression of *GAPDH* mRNA. All reactions were performed in triplicates.

Western blot analyses

After K562-r cells were treated with 8 μM AMN107, 1.5 μM ATO, or the combination of the two, cell lysates were prepared as previously described.[33] In brief, cells were lysed with RIPA buffer (1% NP40, 0.5% deoxycholate, 0.1% SDS, 50 mM Tris-HCl (pH 8.0), and 150 mM sodium chloride) supplemented with complete protease inhibitor cocktail tablets (Roche Applied Science, Germany). Protein concentration was measured by Micro BCA Protein Assay Kit (Pierce, IL). Equal amounts of protein were resolved for Western blot analysis. Primary antibodies were obtained as follows: p-c-abl, c-abl, p-CrkL, p-stat5, c-Fos, p-c-Jun, c-Jun, p-JNK, caspase-7, cleaved caspase-3, cleaved caspase-9, PARP, tublin and actin from Cell Signaling Technology (Beverly, MA), ATF6 from Santa Cruz (CA). Proteins were visualized using Amersham ECL Plus Western Blotting Detection Reagents kit (GE Healthcare, UK) according to the manufacturer's instructions.

Cell cycle analysis

K562-r cells were treated with 1.5 μM ATO, 8 μM AMN107, or the combination of the two for 24 or 48 hrs. Then, cells were harvested, fixed with ice-cold 75% ethanol overnight, stained with 10 μg/mL propidium iodide in PBS containing 0.1 mg/mL RNase A (New England Biolabs, Hertfordshire, UK), and followed with flow cytometry analysis.

Glutathione (GSH) detection assay

The measurement of changes in the GSH level of cell lysates was determined with the Glutathione Apoptosis Assay Kit (Merck KGaA, Darmstadt, Germany). In brief, K562-r cells were treated with 1.5 μM ATO, 8 μM AMN107, or the combination of the two for 3 or 12 hrs, rinsed three times with PBS and harvested. According to the manufacturer's protocol, cells were centrifuged at 700 *g* at 4°C for 5 min, resuspended in ice-cold cell lysis buffer and incubated on ice for 10 min. After centrifugation in a microcentrifuge at 14,000 *g* for 10 mins, the supernatant was transferred to a clean tube and the pellet was discarded. Monochlorobimane Reagent GST was added. After incubation at 37°C for 15–30 mins, the solution was measured using a fluorimeter or fluorescence plate reader with an excitation wavelength of ~380 nm and an emission wavelength of ~460 nm. A negative control sample was prepared by adding only monochlorobimane reagent and cell lysis buffer.

Small interfering RNA transfection

Before transfection of siRNA, cells were washed and resuspended in fresh culture media without antibiotics. siRNA (25 nM) was introduced into cells with program T-003 on the Nucleofector II system (Amaxa, Germany). After transfection, cells were treated with 8 μM AMN107, 1.5 μM ATO, and the combination of the two for 24 hrs and 48 hrs. Cell viability was measured at 24 hr by MTT. The target sequence for JNK-specific siRNA is 5-AAAGAAUGUCCUACCUUCUTT-3. Both the control and JNK-specific siRNAs were obtained from Qiagen (Valencia, CA). Knockdown of JNK expression was confirmed by both RT-PCR and western blot.

Statistical analysis

All data are reported as means ± SEM, and statistical significance was defined as $*p < 0.05$. One-way ANOVA following Student's two-tailed t-tests were used to (SAS Inc., Chicago, IL) evaluate cell growth, viability and apoptosis.

Results

Potent apoptosis induced by AMN107/ATO in imatinib-resistant K562-r cells

K562-r cells have neither BCR-ABL mutation nor its overexpression.[41] Figure 1a and b illustrate the growth inhibitory effects of AMN107, ATO and the combination of the two, under various conditions. Figure 1c demonstrates cell apoptosis induced under conditions as indicated. Although the treatment with ATO or AMN107 alone revealed some effects of growth inhibition, apoptotic effects of these alone treatments appeared to be limited during the observation time period. The most significant apoptotic induction was observed in the cells treated by combining AMN107 with ATO. The apoptosis rate reached to 56.41% at 72 hr in the combinatory treatment group, as compared to 12.23% in ATO and 29.8% in AMN107 alone treatment groups. Detection of mitochondrial transmembrane potential ($\Delta\Psi m$) appeared to show similar results (Figure 1d). Loss of mitochondrial transmembrane potential reached 34.73%

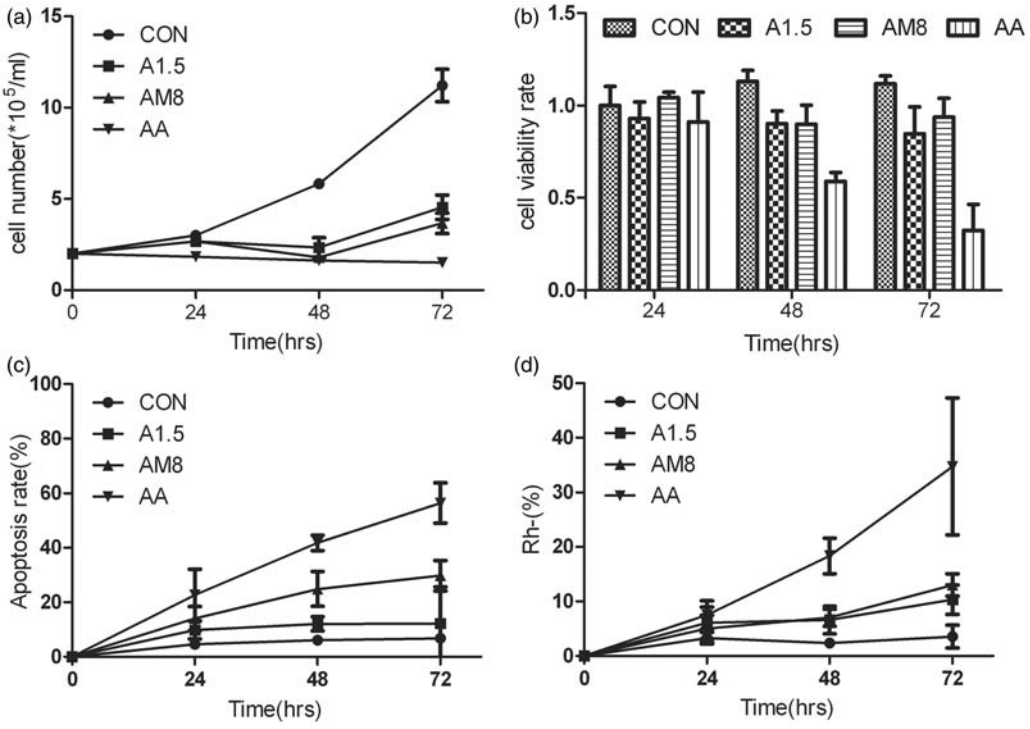

Figure 1 Enhanced cytotoxicity by combined treatment with AMN107 and ATO in K562-r cells. Cells were treated with 1.5 μM ATO (A1.5), 8 μM AMN107 (AM8), or the combination (AA), and were analysed at different time points. The same symbols were used in the following. (a) The cell survival rate was determined by cell counting through trypan blue staining; (b) The cell viability was evaluated by MTT assay; (c) The apoptosis rate was determined through Annexin V–specific antibody and propidium iodide (PI) staining; (d) The loss of mitochondria $\Delta\Psi$m, was evaluated by rhodamine123 and PI double staining. The data are the means $\pm$ SE from three independent experiments

at 72 hr in the combinatory group, as compared to 10.32% in ATO and 13.03% in AMN107 alone treatment groups. Taken together, data shown in Figure 1 demonstrate that ATO significantly potentiated the efficacy of AMN107 to induce apoptosis in imatinib-resistant K562-r cells.

Identification of genes with characteristic expression patterns

Numerous studies have shown that TKIs such as AMN107 interfere with a multitude of signalling pathways which are abnormally perturbed by the BCR-ABL oncoprotein.[17,46,47] ATO is also an agent with extensive effects on intracellular activities.[39] Therefore, it is assumable that mechanisms underlying the apoptosis induced by combining ATO with AMN107 can be far more complex. In an attempt to gain sights into mechanism underlying the synergistic induction of apoptosis, as observed in K562-r cells by combining ATO with AMN107, we applied cDNA microarray analysis, essentially as previously described.[33] In brief, the cells were cultured respectively with the presence of AMN107 (8 μM), ATO (1.5 μM) and the combination of the two, and harvested at the time points of 0, 3, 12, 24, 48 hr. After hybridization and data acquisition, differentially regulated genes were selected through the EDGE-based method.[48] An expression matrix containing expression values of 7158 transcripts across 16 samples (four controls and 12 drug-treated samples) was then constructed. This matrix was then applied to our feature-selection and noise-elimination program (SOM-SVD, Figure S1).[43] The resulting feature-only matrix with expression values of 1441 transcripts across the 12 samples was then subjected to a gene clustering procedure, which revealed nine clusters based on topological relationships (termed clusters 1–9) (see Figure S2). CPPs were used to display sample-specific transcriptome changes to facilitate direct comparisons among three groups (Figure 2a). Real-time RT-PCR assay was performed on a number of randomly selected genes, represented by *EGR1, FOXO3* and *HSPA5,* as an independent validation of the array data (Figure 2c).

Interestingly, changes in the transcriptome patterns observed in 8 μM AMN107 (Am8) series shared some similarity to the patterns observed in 1.5 μM ATO treatment (A1.5) series, which appeared to somewhat depict the patterns observed in the co-treatment series throughout the time course (Figure 2a). Then, we compared the number of regulated genes (based on 2-fold change threshold) among the three types of treatment series (Table 1). It appeared that the number of regulated genes in the co-treatment series was much larger than that either in ATO or AMN107 alone treatment series. Also, the number of up-regulated genes appeared to be much larger than that of down-regulated ones, implicating the occurrence of strong cellular stress. Four gene clusters with the most pronounced differences were then viewed in the hierarchical structure, displaying synergetic patterns in the co-treatment series, as those displayed in SOM-SVD analysis, Gene involved in these patterns were typically represented by those coding metabolism related enzymes, endoplasmic reticulum (ER)

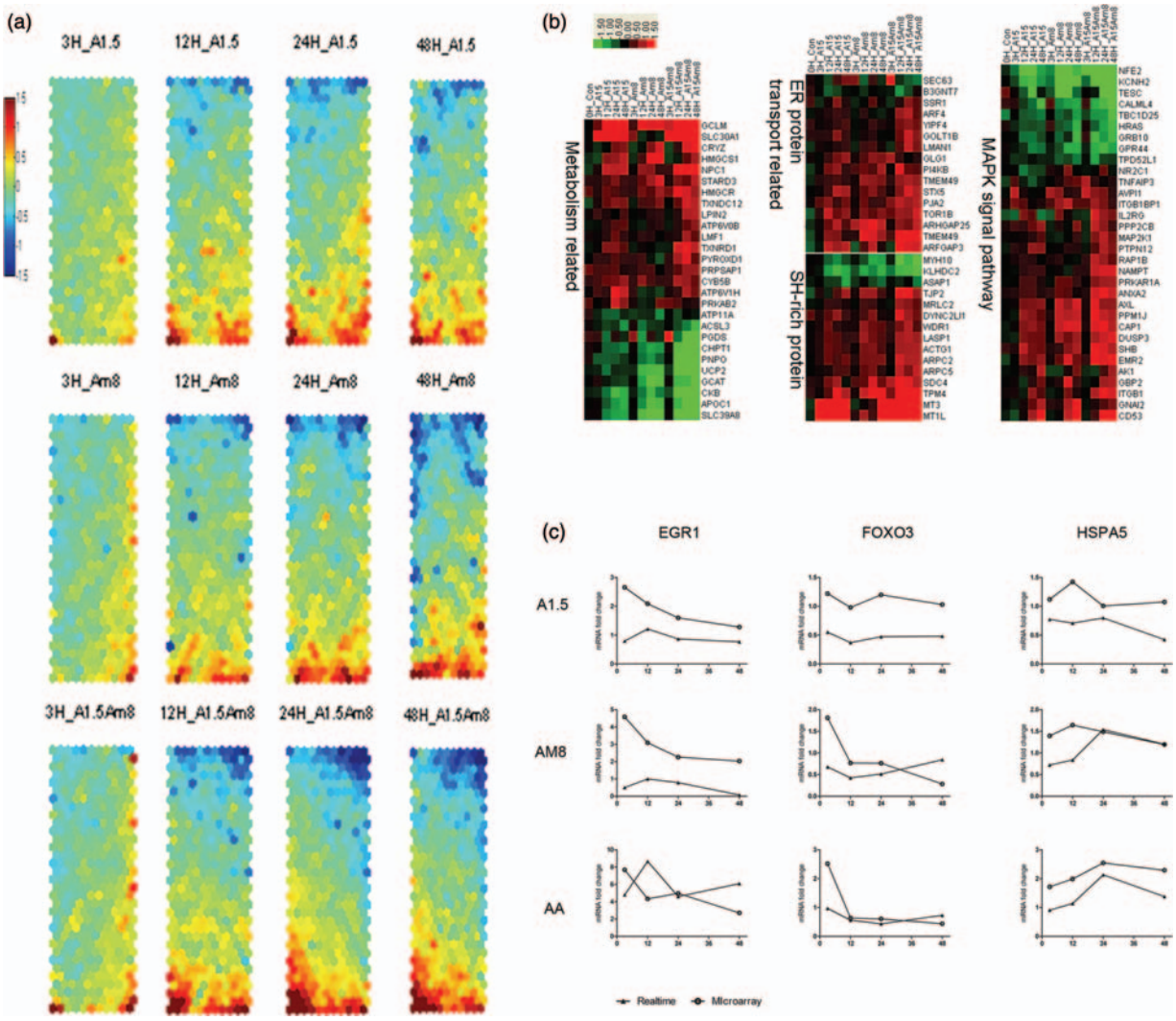

Figure 2 CPP-SOM of microarray data. The time-course transcriptomes (0, 3, 12, 24, 48 hr) of K562-r cells treated with 1.5 μM ATO (A1.5), 8 μM AMN107 (AM8), or the combination (AA) were illustrated. (a) CPP-SOM of microarray data output. Each presentation illustrated a sample-specific transcriptome map, in which all the up-regulated (in red), down-regulated (in blue), and moderately regulated (in yellow and green) genes were well delineated. Colour index stands for log ratio with base 2; (b) Four major regulatory categories were recognizable in the above and summarized as modulated gene clusters; (c) The fidelity of microarray data was validated by quantitative RT-PCR of randomly chosen genes, represented by *EGR1*, *FOXO3* and *HSPA5*. The data are the means ± SE from three independent experiments

Table 1 Differentially expressed genes in microarray analysis

	Up-regulated gene numbers			Down-regulated gene number		
Time (h)	**A1.5**	**Am8**	**AA**	**A1.5**	**Am8**	**AA**
3	12	20	47	1	6	6
12	61	60	131	8	28	87
24	64	99	203	12	48	138
48	70	89	203	26	87	137

Differentially expressed genes are screened based on a two-fold change threshold.

transport proteins, proteins rich in sulphydryl group and members in MAPK signalling pathways. Obviously, of the regulated genes are involved in a broad field of cellular processes, indicating that massive cellular responses occurred prior to the final stage of the apoptosis (Figure 2b).

During the time period of 3–12 hr, the number of genes modulated by AMN107 was relatively small and these regulated genes were largely represented by those involved in downstream of TK (e.g. *GPR44, PLK3, DUSP3*) (All mentioned genes were indicated in Supplementary Figure S3.). Up-regulated genes in ATO-treated series were largely restricted to those encoding proteins of the metallothionein family, mitochondria respiratory complexes, unfold protein response (UPR) and those involved in the GSH redox system (e.g. *MT1G, NQO1, TOMM34, HSPA5, GCLM*), strongly suggesting the occurrence of UPR. Genes regulated in the co-treatment series were largely overlapped with those regulated in ATO or/and AMN107 series, and some of them appeared to be enhanced, in terms of their fold changes (e.g. *ITGB3BP, GABRB3, CDKN1A*). In the intermediate stage (24 hr), transcriptome changes in the co-treatment series were more dramatic, typically highlighted by genes encoding ER proteins as well as ER stress markers,

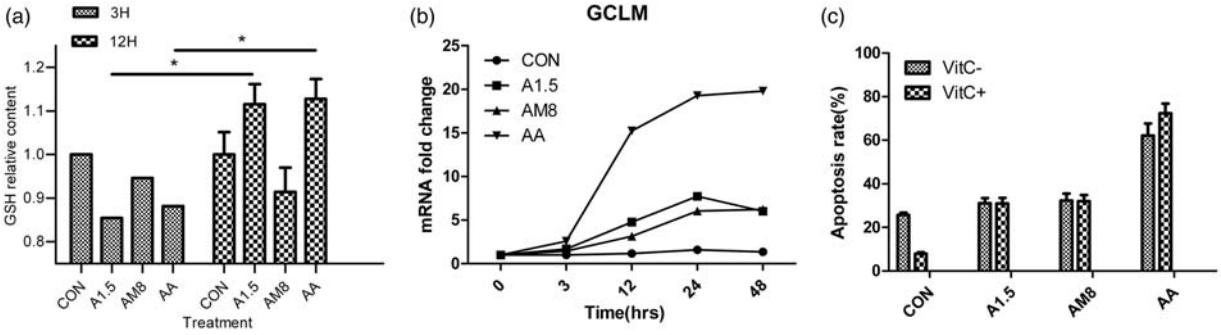

Figure 3 Glutathione redox system of K562-r cells related to the rescue response of oxidative stress. (a) GSH levels in K562-r cells after the treatments were detected in early and late stage. Untreated K562-r cells were used as standard control. *, $p < 0.05$ denotes the statistically significant level of difference between ATO alone treated group or the combined ATO and AMN107 group at 12 hr with at 3 hr respectively; (b) mRNA level of *GCLM* in K562-r cells after the treatments were detected at 12 hr. (c) The apoptosis rate was determined through Annexin V-specific antibody and propidium iodide (PI) staining. K562-r cells were treated with 1.5 μM ATO, 8 μM AMN107, or the combination for 48 hr and then cells were collected and evaluated. VitC+, 10 mM vitamin C was added at 2 hr before the treatments. The data are the means ± SE from three independent experiments

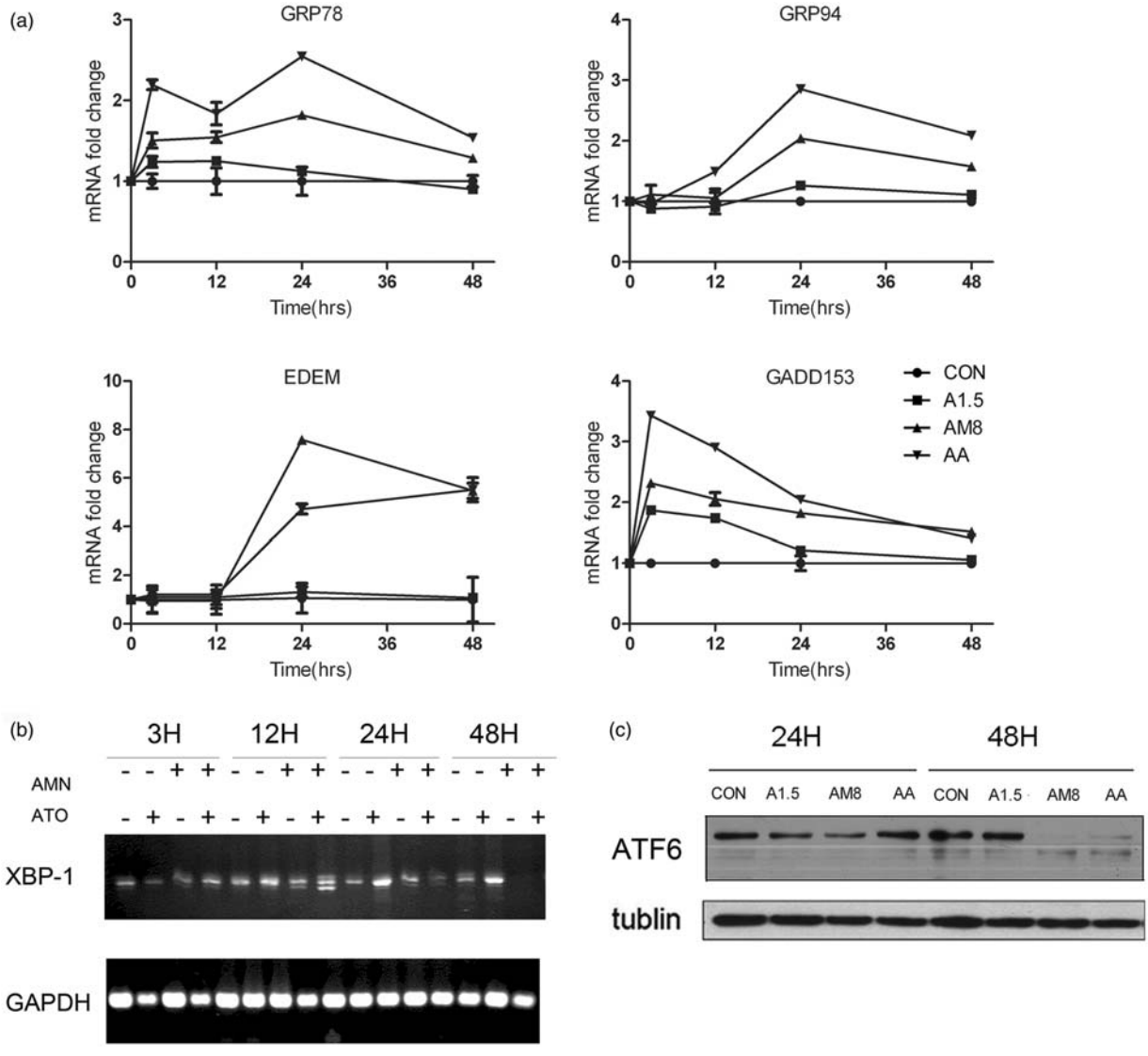

Figure 4 Persistent ER stress involved in initiating apoptosis in K562-r cells. (a) Real-time RT-PCR detected four ER stress markers in K562-r cells at a series of time points (0, 3, 12, 24, 48 hr). The data are the means ± SE from three independent experiments; (b) ER stress-induced alternative splicing of *XBP1* mRNA was detected using RT-PCR and products were separated by electrophoresis on 2% agarose gel. *GAPDH* was as a housekeeping gene for loading control; (c) Protein level of ATF6 was analysed by Western blotting and tubulin was as the loading control

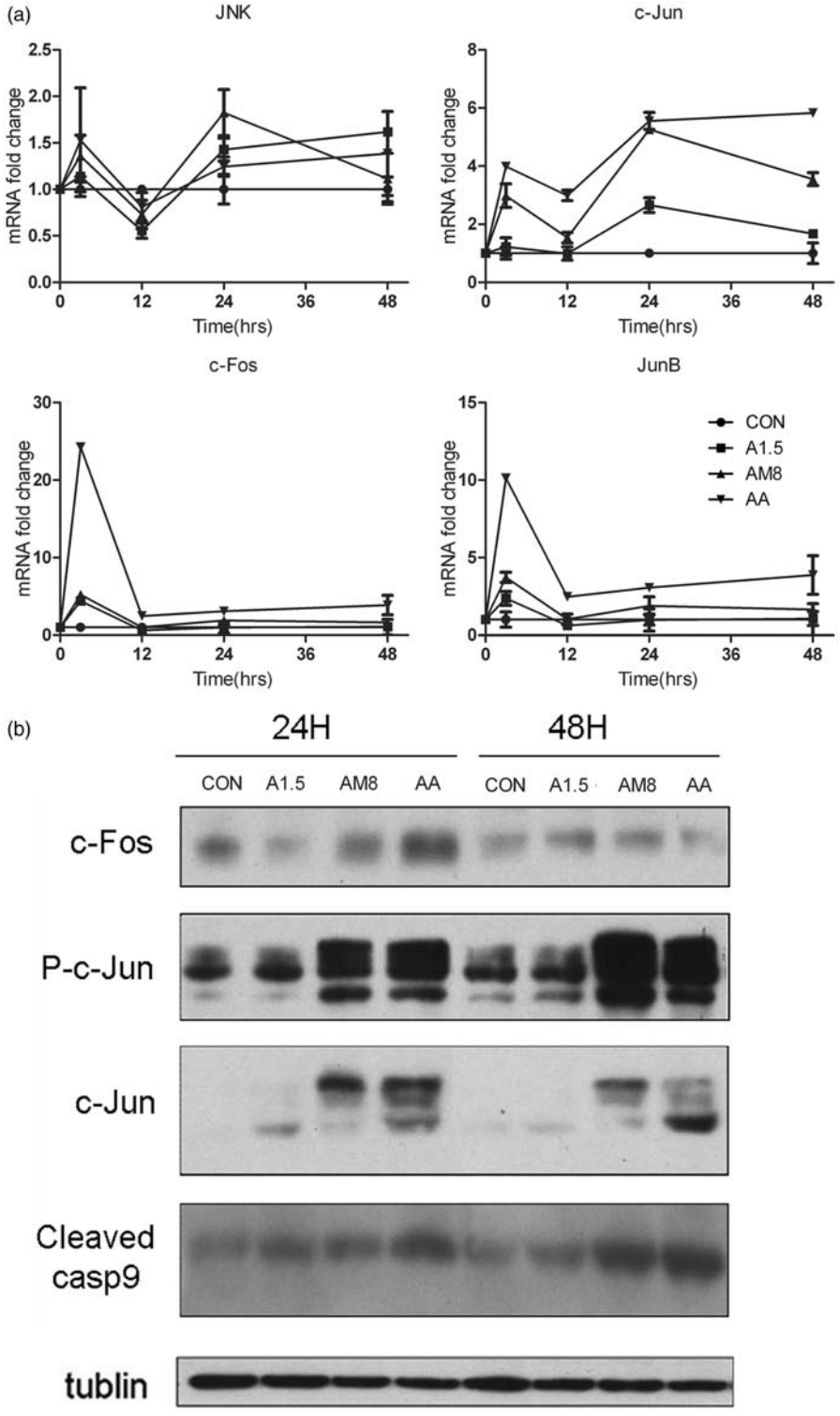

Figure 5 ER stress induced apoptosis in K562-r cells via SAPK/JNK signalling cascades. (a) Real-time RT-PCR detected four JNK-pathway members in K562-r cells at a series of time points (0, 3, 12, 24, 48 hr). The data are the means ± SE from three independent experiments; (b) Protein levels of c-Fos, c-Jun, p-c-Jun and the cleaved caspase-9 fragment were analysed by western blotting and tubulin was as the loading control

such as *HSPA5, EDEM1, ATF6*, and *DDIT3*. Later at 48 h, transcriptome changes were more focused on the process of cell death, as highlighted by down-regulation of metabolism, cytoskeleton proteins and respiration complexes (e.g. *NQO1, NGFRAP1, NME1* and *PGDS*), indicating the mitochondrial dysfunction and irreversible ongoing apoptosis.

ATO promoted rescue response of oxidative stress related to the GSH redox system

Genes encoding oxido-reductases were up-regulated in ATO alone and the co-treatment series. Also, genes encoding members of the metallothionein family were up-regulated in these treatment series. Oxido-reductases

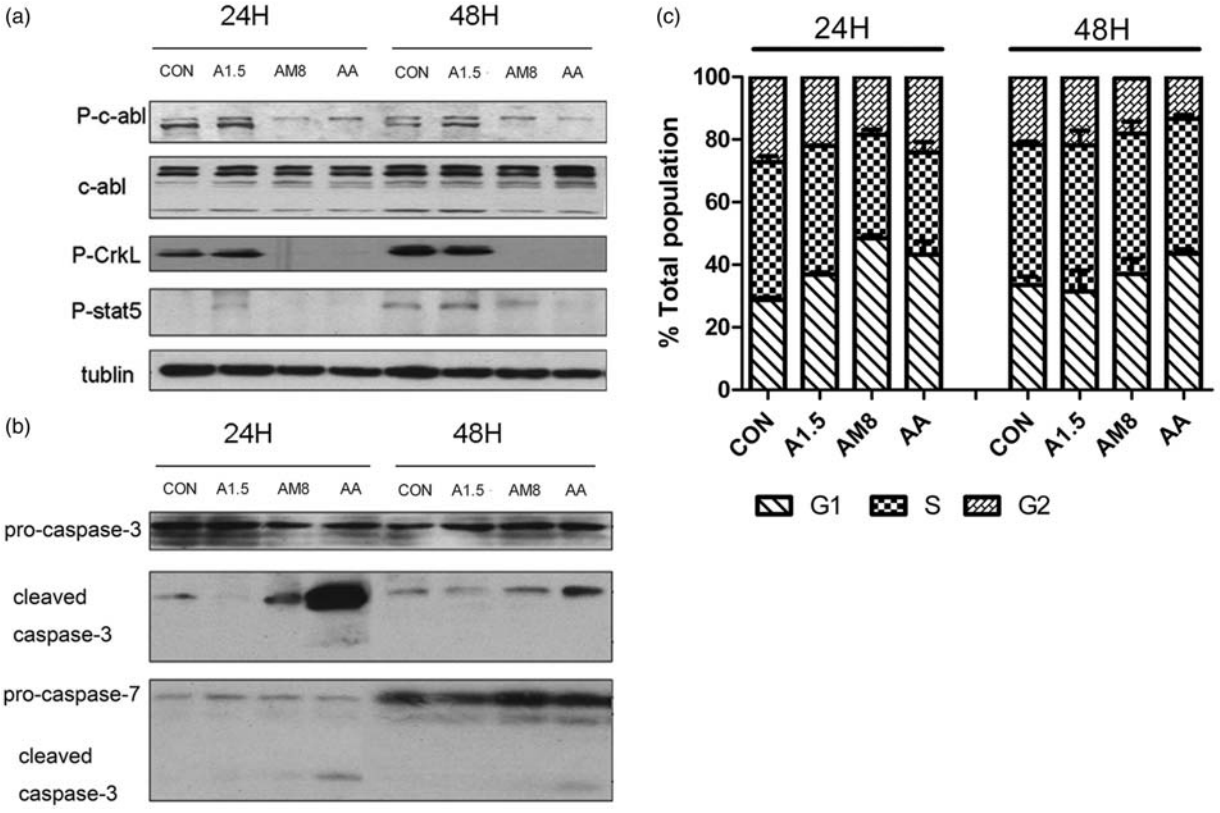

Figure 6 Apoptosis initiated by the caspase-dependent pathway but not by cell cycle arrest in K562-r cells with ATO plus AMN107. (a) cell lysates were analysed by western blot with antibodies against phosphorylated BCR-ABL (p-abl), total c-abl, phosphorylated CrkL (p-CrkL), phosphorylated stat5 (p-stat5). Tubulin was as a loading control in this and the following western blotting experiments. (b) Caspase effectors and their cleaved fragments were detected by western blot. (c) Alterations in cell cycle progression were evaluated by flow cytometry analysis. K562-r cells were treated with 1.5 μM ATO, 8 μM AMN107, or the combination for 24, or 48 hr. Cell cycle phase distributions are the means $\pm$ SE from three independent experiments

are associated with the GSH redox system and the respiratory chains, and members of the metallothionein family are involved in the redox-buffering system. As shown in Figure 3 and the microarray profile, the metallothionein family was up-regulated since the early stage of ATO and co-treatments when apoptosis did not initiated, coupled with GSH level greatly reduced at 3 hr. Because the metallothionein family transcription increased in the feedback response to the ATO-causing oxidative stress in K562-r cells, the GSH level was up again at 12 hr. Glutamate-cysteine ligase modifier subunit (GCLM) was up-regulated significantly at 12 hr, closely related to the uprising of GSH level (Figure 3a and b). It was therefore deducible that multiple systems for buffering oxidative stress were activated in ATO alone and the co-treatment series in order to prevent extensive damage caused by oxidative stress. For example, glutamate cysteine ligase (GCL) is a rate-limiting enzyme in GSH biosynthesis and the increase in GCL alone is sufficient to activate GSH biosynthesis.[49] On the other hand, the above data might also explicate why cellular levels of ROS were not changed either in ATO or AMN107 treatment series (data available upon request). Together with the data that vitamin C failed to stop the apoptotic process triggered by ATO or the co-treatment, it is logical to assume that these treatments triggered cellular oxidative stress, and promoted the rescue of redox homeostasis in cells by activating multiple redox-buffering systems. However, due to the nature of cancer cells, probably with damaged redox homeostasis, the cells were inevitably under the apoptosis.

Potent apoptosis accomplished through ER-stress

ER is the first intracellular compartment for posttranslational modifications, such as glycosylation and disulphide bond formation, depending on the highly oxidizing environment existing within the ER (GSH:GSSG $\sim$ 3:1), as compared to the reducing conditions of the cytosol. Unbalanced GSH redox system can spoil the ER environment, inhibit protein disulphide bond formation and result in ER stress, which in turn can cause subsequent cellular responses, either to recover normal homeostasis or to initiate cell apoptosis.[50–52] In this setting, however, cell death via ER stress mediated apoptosis is strongly evident, as highlighted by up-regulation of ER stress markers, such as *GRP78, GADD153* and *EDEM,* (Figure 4a),[53] and by the early-stage spliced *XBP-1*, a transducer of ER-stress, and the late-stage activated ATF6 (Figures 4b and c).[54] Members of the JNK pathway are thought to bridge ER stress response and apoptosis.[55,56] The up-regulated c-Jun and its partner c-Fos protein, as well as their mRNA, indicated that the JNK pathway indeed played a role in mediating apoptosis in this setting (Figure 5).

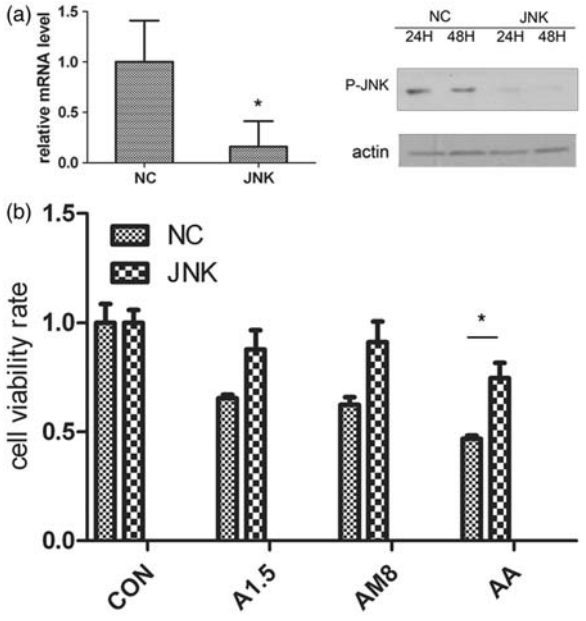

Figure 7 JNK interference partially improved cell viability of drug-treated groups in K562-r cells. (a) K562-r cells were transfected with control siRNA or JNK-specific siRNA. After 72 hrs of culture, JNK mRNA expression was determined by real-time RT-PCR. The functional protein level was detected at 24 hr and 48 hr after transfection. After siRNA transfection, *JNK* mRNA expression was determined by real-time RT-PCR at 72 hr and the functional protein p-JNK was detected by western blot at 24 hr and 48 hr (upper panel), *, $p < 0.05$ denotes the statistically significant level of difference between siRNA transfection with the non-target siRNA control (NC). Actin is used as a loading control. (b) The viability of NC and JNK siRNA-transfected cells treated with 1.5 μM ATO (A1.5), 8 μM AMN107 (AM8), or the combination (AA) for 24 hrs was determined by MTT assay. NC denotes cell viability of non-siRNA-transfected cells as 100%. *, $p < 0.05$ denotes the statistically significant level of difference between NC with siRNA-transfected cells treatment group

Apoptosis initiated by the caspase-dependent pathway but not by cell cycle arrest in K562-r cells co-treated with AMN107 and ATO

These were the typical TKI key features such as down-regulation of phosphorylation of c-abl, CrkL and stat5, members of downstream of BCR-ABL that showed in AMN107 and co-treatment series (Figure 6a). Data shown in Figure 6b indicate the occurrence of caspase-dependent apoptosis in the co-treatment series. Remarkably, increased cleavage of caspase-3 and caspase-7 were detected in the cells. The JNK pathway-bridged apoptosis was confirmed with small interfering RNA targeting JNK (Figure 7). The shut-down of JNK abrogated the synergistic induction of apoptosis in the combination treatment group, which indicated that the synergic effects of the co-treatment were primarily mediated through the JNK signalling pathway.

Previous studies showed that ATO induced G2/M arrest through activation of p53. Cell cycle-arrest in the G0/G1 phase was also reported in some regulatory T cells treated with AMN107.[57,58] K562-r cells, as the parental K562 cells, are p53-deficient. In this study, however, ATO failed to interfere with cell cycle progression, as compared to untreated control group. Interestingly, 8 μM AMN107 appeared to somewhat lead to cycle arrest at the G1 phase at 24 hr but not at 48 hr. In the co-treatment series, a minor accumulation of the cells in the G1 phase appeared to be evident at 24 hr (Figure 6c), which was probably due to the effect of AMN107, whereas cell arrest was not detectable at 48 hr. Thus, it was deducible that the cytotoxic effect of the co-treatment with AMN107 and ATO on K562-r cells was primarily due to cell apoptosis rather than cell arrest.

Discussion

AMN107, a second-generation TKI, has significantly improved the efficacy of TKI in CML. In particular, AMN107 is superior to imatinib for the treatment of chronic-phase CML patients.[22] However, recent studies have raised questions whether TKI alone can completely eradicate CML cells, particularly with respect to those CML patients with BCR–ABL independent imatinib-resistance.[59] In this study, we showed that ATO could significantly potentiate the efficacy of AMN107 in BCR–ABL independent imatinib-resistant K562-r cells. We identified that the cytotoxicity synergistically generated by AMN107 with ATO was the induction of cell apoptosis rather than cell arrest. The transcriptome and molecular data indicated that the apoptosis was caspase dependent and triggered by oxidative stress/ER stress. We also confirmed that the JNK signalling bridged ER stress and the apoptosis. In addition, ATO may play a dual role in K562-r cells. On one hand, it triggered oxidative stress, and on the other hand, it stimulated the multiple cellular systems to restore cellular homeostasis caused by oxidative stress. However, due to impaired buffer/repairs systems in the co-treatment group, the apoptosis appeared to be inevitable.

Previously, ATO alone was able to induce pre-apoptotic events such as cytosolic cytochrome C accumulation and caspase activation at appropriate concentrations in various cancer cell lines.[60] In imatinib-sensitive K562 cells, ATO also induced ER stress-mediated pathway of cell apoptosis.[33] However, under our experimental conditions, lower concentration of ATO at a relatively short treatment interval (0–72 hr) did not induce significant apoptosis and decrease of BCR-ABL protein level; only the combination of ATO with AMN107 was capable of inducing the significant apoptosis in K562-r cells (Figure 1 and Figure 6a). Probably, ATO potentiated the efficacy of AMN107 by activating ER stress and UPR, which eventually led to cell apoptosis. It was reported that GSH antagonized the apoptotic effect of ATO, either through conjugating ATO or by sequestering reactive oxygen induced by ATO.[61] In this setting, however, data showed that intracellular levels of GSH were largely restored in the co-treatment series at 12 hr. Instead of survival rescue, the cells underwent apoptosis. A possible explanation for such phenomenon was that the program of ER stress-mediated apoptosis was already started at the early stage (i.e. at 3 hr) of the treatment, although several reports showed the interplay between oxidative stress and ER stress-mediated apoptosis.[62,52] Mechanistic link between them remained to be investigated. However, our research model, i.e. K562-r cells co-treated with AMN107 and ATO, may provide a roadmap to conduct such investigation effectively and efficiently in near future.

In conclusion, we demonstrated that ATO synergistically potentiated the apoptotic efficacy of the TKI AMN107 in imatinib-resistant CML cell line K562-r. The results obtained in this report highlighted the potential of successful combination of oxidative compounds with a TKI as an effective strategy in treating imatinib-resistant CML.

Author contributions: All authors participated in the design of the studies, interpretation of the studies and analysis of the data and reviewing of the manuscript. YX conducted the experiments, HF analysed the transcriptome data, YX, JZ and YZD wrote the manuscript.

ACKNOWLEDGEMENTS

This work was supported in part by grants from the National Natural Science Foundation (81170503 and 90919059), Chinese Academy of Sciences (KSCX2-EW-Q-1-08), Ministry of Science and Technology of China (2013CB966802 and 2009CB825607), the Shanghai Commission of Science and Technology (11431922402) and SA-SIBS Scholarship Program (YZD).

REFERENCES

1. Shtivelman E, Lifshitz B, Gale RP, Canaani E. Fused transcript of abl and bcr genes in chronic myelogenous leukaemia. *Nature* 1985;**315**:550–4
2. Goldman JM, Melo JV. Targeting the bcr-abl tyrosine kinase in chronic myeloid leukemia. *N Engl J Med* 2001;**344**:1084–6
3. Druker BJ, Lydon NB. Lessons learned from the development of an abl tyrosine kinase inhibitor for chronic myelogenous leukemia. *J Clin Invest* 2000;**105**:3–7
4. Baccarani M, Saglio G, Goldman J, Hochhaus A, Simonsson B, Appelbaum F, Apperley J, Cervantes F, Cortes J, Deininger M, Gratwohl A, Guilhot F, Horowitz M, Hughes T, Kantarjian H, Larson R, Niederwieser D, Silver R, Hehlmann R. Evolving concepts in the management of chronic myeloid leukemia: recommendations from an expert panel on behalf of the european leukemianet. *Blood* 2006;**108**:1809–20
5. Baccarani M, Cortes J, Pane F, Niederwieser D, Saglio G, Apperley J, Cervantes F, Deininger M, Gratwohl A, Guilhot F, Hochhaus A, Horowitz M, Hughes T, Kantarjian H, Larson R, Radich J, Simonsson B, Silver RT, Goldman J, Hehlmann R. Chronic myeloid leukemia: An update of concepts and management recommendations of European leukemianet. *J Clin Oncol* 2009;**27**:6041–51
6. Hochhaus A, O'Brien SG, Guilhot F, Druker BJ, Branford S, Foroni L, Goldman JM, Muller MC, Radich JP, Rudoltz M, Mone M, Gathmann I, Hughes TP, Larson RA. Six-year follow-up of patients receiving imatinib for the first-line treatment of chronic myeloid leukemia. *Leukemia* 2009;**23**:1054–61
7. de Lavallade H, Apperley JF, Khorashad JS, Milojkovic D, Reid AG, Bua M, Szydlo R, Olavarria E, Kaeda J, Goldman JM, Marin D. Imatinib for newly diagnosed patients with chronic myeloid leukemia: Incidence of sustained responses in an intention-to-treat analysis. *J Clin Oncol* 2008;**26**:3358–63
8. Bixby D, Talpaz M. Seeking the causes and solutions to imatinib-resistance in chronic myeloid leukemia. *Leukemia* 2011;**25**:7–22
9. Gorre ME, Mohammed M, Ellwood K, Hsu N, Paquette R, Rao PN, Sawyers CL. Clinical resistance to sti-571 cancer therapy caused by bcr-abl gene mutation or amplification. *Science* 2001;**293**:876–80
10. O'Hare T, Eide CA, Deininger MW. Bcr-abl kinase domain mutations, drug resistance, and the road to a cure for chronic myeloid leukemia. *Blood* 2007;**110**:2242–9
11. Dulucq S, Bouchet S, Turcq B, Lippert E, Etienne G, Reiffers J, Molimard M, Krajinovic M, Mahon FX. Multidrug resistance gene (mdr1) polymorphisms are associated with major molecular responses to standard-dose imatinib in chronic myeloid leukemia. *Blood* 2008;**112**:2024–7
12. White DL, Saunders VA, Dang P, Engler J, Zannettino AC, Cambareri AC, Quinn SR, Manley PW, Hughes TP. Oct-1-mediated influx is a key determinant of the intracellular uptake of imatinib but not nilotinib (amn107): reduced oct-1 activity is the cause of low in vitro sensitivity to imatinib. *Blood* 2006;**108**:697–704
13. Wang L, Giannoudis A, Lane S, Williamson P, Pirmohamed M, Clark RE. Expression of the uptake drug transporter hoct1 is an important clinical determinant of the response to imatinib in chronic myeloid leukemia. *Clin Pharmacol Ther* 2008;**83**:258–64
14. Ptasznik A, Nakata Y, Kalota A, Emerson SG, Gewirtz AM. Short interfering rna (sirna) targeting the lyn kinase induces apoptosis in primary, and drug-resistant, bcr-abl1(+) leukemia cells. *Nature Med* 2004;**10**:1187–9
15. Wu J, Meng F, Lu H, Kong L, Bornmann W, Peng Z, Talpaz M, Donato NJ. Lyn regulates bcr-abl and gab2 tyrosine phosphorylation and c-cbl protein stability in imatinib-resistant chronic myelogenous leukemia cells. *Blood* 2008;**111**:3821–9
16. Meyn 3rd MA, Wilson MB, Abdi FA, Fahey N, Schiavone AP, Wu J, Hochrein JM, Engen JR, Smithgall TE. Src family kinases phosphorylate the bcr-abl sh3-sh2 region and modulate bcr-abl transforming activity. *J Biol Chem* 2006;**281**:30907–16
17. Weisberg E, Manley PW, Breitenstein W, Bruggen J, Cowan-Jacob SW, Ray A, Huntly B, Fabbro D, Fendrich G, Hall-Meyers E, Kung AL, Mestan J, Daley GQ, Callahan L, Catley L, Cavazza C, Azam M, Neuberg D, Wright RD, Gilliland DG, Griffin JD. Characterization of amn107, a selective inhibitor of native and mutant bcr-abl. *Cancer cell* 2005;**7**:129–41
18. Rosti G, Castagnetti F, Gugliotta G, Palandri F, Martinelli G, Baccarani M. Dasatinib and nilotinib in imatinib-resistant philadelphia-positive chronic myelogenous leukemia: A 'head-to-head comparison'. *Leuk Lymphoma* 2010;**51**:583–91
19. Zhou L, Meng F, Yin O, Wang J, Wang Y, Wei Y, Hu P, Shen Z. Nilotinib for imatinib-resistant or -intolerant chronic myeloid leukemia in chronic phase, accelerated phase, or blast crisis: A single- and multiple-dose, open-label pharmacokinetic study in chinese patients. *Clin Ther* 2009;**31**:1568–75
20. Saglio G, Kim DW, Issaragrisil S, le Coutre P, Etienne G, Lobo C, Pasquini R, Clark RE, Hochhaus A, Hughes TP, Gallagher N, Hoenekopp A, Dong M, Haque A, Larson RA, Kantarjian HM. Nilotinib versus imatinib for newly diagnosed chronic myeloid leukemia. *N Engl J Med* 2010;**362**:2251–9
21. Swords R, Mahalingam D, Padmanabhan S, Carew J, Giles F. Nilotinib: optimal therapy for patients with chronic myeloid leukemia and resistance or intolerance to imatinib. *Drug Des Devel Ther* 2009;**3**:89–101
22. Kantarjian HM, Hochhaus A, Saglio G, De Souza C, Flinn IW, Stenke L, Goh YT, Rosti G, Nakamae H, Gallagher NJ, Hoenekopp A, Blakesley RE, Larson RA, Hughes TP. Nilotinib versus imatinib for the treatment of patients with newly diagnosed chronic phase, philadelphia chromosome-positive, chronic myeloid leukaemia: 24-month minimum follow-up of the phase 3 randomised enestnd trial. *Lancet Oncol* 2011;**12**:841–51
23. Valent P, Gastl G, Geissler K, Greil R, Hantschel O, Lang A, Linkesch W, Lion T, Petzer AL, Pittermann E, Pleyer L, Thaler J, Wolf D. Nilotinib as frontline and second-line therapy in chronic myeloid leukemia: Open questions. *Crit Rev Oncol Hematol* 2012;**82**:370–7
24. Ibrahim AR, Clark RE, Holyoake TL, Byrne J, Shepherd P, Apperley JF, Milojkovic D, Szydlo RM, Goldman JM, Marin D. Second generation tyrosine kinase inhibitors improve the survival of patients with chronic myeloid leukemia who have failed imatinib therapy. *Haematologica* 2011;**96**:1779–82
25. Guilhot F, Gardembas M, Rousselot P, Tulliez M, Vigier M, Buzyn A, Rigal-Huguet F, Legros L, Michallet M, Berthou C, Najman A, Maloisel F, Mahon FX, Facon T, Berthaud P, Guilhot J. Imatinib in combination with cytarabine for the treatment of philadelphia-positive chronic myelogenous leukemia chronic-phase patients: rationale and design of phase i/ii trials. *Semin Hematol* 2003;**40**:92–7

26. Voglova J, Maisnar V, Beranek M, Chrobak L. [combination of imatinib and anagrelide in treatment of chronic myeloid leukemia in blastic phase]. *Vnitr Lek* 2006;**52**:819–22
27. Antman KH. Introduction: the history of arsenic trioxide in cancer therapy. *Oncologist* 2001;**6**:1–2
28. Soignet SL, Frankel SR, Douer D, Tallman MS, Kantarjian H, Calleja E, Stone RM, Kalaycio M, Scheinberg DA, Steinherz P, Sievers EL, Coutre S, Dahlberg S, Ellison R, Warrell Jr RP. United states multicenter study of arsenic trioxide in relapsed acute promyelocytic leukemia. *J Clin Oncol* 2001;**19**:3852–60
29. Miller Jr WH, Schipper HM, Lee JS, Singer J, Waxman S. Mechanisms of action of arsenic trioxide. *Cancer Res* 2002;**62**:3893–903
30. Carney DA. Arsenic trioxide mechanisms of action–looking beyond acute promyelocytic leukemia. *Leuk Lymphoma* 2008;**49**:1846–51
31. Shim MJ, Kim HJ, Yang SJ, Lee IS, Choi HI, Kim T. Arsenic trioxide induces apoptosis in chronic myelogenous leukemia k562 cells: possible involvement of p38 map kinase. *J Biochem Mol Biol* 2002;**35**:377–83
32. Nimmanapalli R, Bali P, O'Bryan E, Fuino L, Guo F, Wu J, Houghton P, Bhalla K. Arsenic trioxide inhibits translation of mrna of bcr-abl, resulting in attenuation of bcr-abl levels and apoptosis of human leukemia cells. *Cancer Res* 2003;**63**:7950–8
33. Du Y, Wang K, Fang H, Li J, Xiao D, Zheng P, Chen Y, Fan H, Pan X, Zhao C, Zhang Q, Imbeaud S, Graudens E, Eveno E, Auffray C, Chen S, Chen Z, Zhang J. Coordination of intrinsic, extrinsic, and endoplasmic reticulum-mediated apoptosis by imatinib mesylate combined with arsenic trioxide in chronic myeloid leukemia. *Blood* 2006;**107**:1582–90
34. Zhang QY, Mao JH, Liu P, Huang QH, Lu J, Xie YY, Weng L, Zhang Y, Chen Q, Chen SJ, Chen Z. A systems biology understanding of the synergistic effects of arsenic sulfide and imatinib in bcr/abl-associated leukemia. *Proc Natl Acad Sci USA* 2009;**106**:3378–83
35. Lu J, Chew EH, Holmgren A. Targeting thioredoxin reductase is a basis for cancer therapy by arsenic trioxide. *Proc Natl Acad Sci USA* 2007;**104**:12288–93
36. Emadi A, Gore SD. Arsenic trioxide - an old drug rediscovered. *Blood Rev* 2010;**24**:191–9
37. Kitchin KT, Conolly R. Arsenic-induced carcinogenesis–oxidative stress as a possible mode of action and future research needs for more biologically based risk assessment. *Chem Res Toxicol* 2010;**23**:327–35
38. Kumar P, Gao Q, Ning Y, Wang Z, Krebsbach PH, Polverini PJ. Arsenic trioxide enhances the therapeutic efficacy of radiation treatment of oral squamous carcinoma while protecting bone. *Mol Cancer Ther* 2008;**7**:2060–9
39. Gazitt Y, Akay C. Arsenic trioxide: an anti cancer missile with multiple warheads. *Hematology* 2005;**10**:205–13
40. Yi J, Yang J, He R, Gao F, Sang H, Tang X, Ye RD. Emodin enhances arsenic trioxide-induced apoptosis via generation of reactive oxygen species and inhibition of survival signaling. *Cancer Res* 2004;**64**:108–16
41. Mahon FX, Deininger MW, Schultheis B, Chabrol J, Reiffers J, Goldman JM, Melo JV. Selection and characterization of bcr-abl positive cell lines with differential sensitivity to the tyrosine kinase inhibitor sti571: diverse mechanisms of resistance. *Blood* 2000;**96**:1070–9
42. Zheng PZ, Wang KK, Zhang QY, Huang QH, Du YZ, Zhang QH, Xiao DK, Shen SH, Imbeaud S, Eveno E, Zhao CJ, Chen YL, Fan HY, Waxman S, Auffray C, Jin G, Chen SJ, Chen Z, Zhang J. Systems analysis of transcriptome and proteome in retinoic acid/arsenic trioxide-induced cell differentiation/apoptosis of promyelocytic leukemia. *Proc Natl Acad Sci USA* 2005;**102**:7653–8
43. Xiao L, Wang K, Teng Y, Zhang J. Component plane presentation integrated self-organizing map for microarray data analysis. *FEBS Lett* 2003;**538**:117–24
44. Mi H, Guo N, Kejariwal A, Thomas PD. Panther version 6: Protein sequence and function evolution data with expanded representation of biological pathways. *Nucleic Acids Res* 2007;**35**:D247–52
45. Goh KI, Cusick ME, Valle D, Childs B, Vidal M, Barabasi AL. The human disease network. *Proc Natl Acad Sci USA* 2007;**104**:8685–90
46. Weisberg E, Manley P, Mestan J, Cowan-Jacob S, Ray A, Griffin JD. Amn107 (nilotinib): a novel and selective inhibitor of bcr-abl. *Br J Cancer* 2006;**94**:1765–9
47. Kantarjian H, Giles F, Wunderle L, Bhalla K, O'Brien S, Wassmann B, Tanaka C, Manley P, Rae P, Mietlowski W, Bochinski K, Hochhaus A, Griffin JD, Hoelzer D, Albitar M, Dugan M, Cortes J, Alland L, Ottmann OG. Nilotinib in imatinib-resistant cml and philadelphia chromosome-positive all. *N Engl J Med* 2006;**354**:2542–51
48. Storey JD, Xiao W, Leek JT, Tompkins RG, Davis RW. Significance analysis of time course microarray experiments. *Proc Natl Acad Sci USA* 2005;**102**:12837–42
49. Chen Y, Shertzer HG, Schneider SN, Nebert DW, Dalton TP. Glutamate cysteine ligase catalysis: Dependence on atp and modifier subunit for regulation of tissue glutathione levels. *J Biol Chem* 2005;**280**:33766–74
50. Townsend DM. S-glutathionylation: indicator of cell stress and regulator of the unfolded protein response. *Mol Interv* 2007;**7**:313–24
51. Yang G, Yang W, Wu L, Wang R. H2s, endoplasmic reticulum stress, and apoptosis of insulin-secreting beta cells. *J Biol Chem* 2007;**282**:16567–76
52. Frosali S, Leonini A, Ettorre A, Di Maio G, Nuti S, Tavarini S, Di Simplicio P, Di Stefano A. Role of intracellular calcium and s-glutathionylation in cell death induced by a mixture of isothiazolinones in hl60 cells. *Biochim Biophys Acta* 2009;**1793**:572–83
53. Ni M, Lee AS. Er chaperones in mammalian development and human diseases. *FEBS Lett* 2007;**581**:3641–51
54. Lee AH, Iwakoshi NN, Glimcher LH. Xbp-1 regulates a subset of endoplasmic reticulum resident chaperone genes in the unfolded protein response. *Mol Cell Biol* 2003;**23**:7448–59
55. Urano F, Wang X, Bertolotti A, Zhang Y, Chung P, Harding HP, Ron D. Coupling of stress in the er to activation of jnk protein kinases by transmembrane protein kinase ire1. *Science* 2000;**287**:664–6
56. Tournier C, Hess P, Yang DD, Xu J, Turner TK, Nimnual A, Bar-Sagi D, Jones SN, Flavell RA, Davis RJ. Requirement of jnk for stress-induced activation of the cytochrome c-mediated death pathway. *Science* 2000;**288**:870–4
57. Han YH, Kim SZ, Kim SH, Park WH. Arsenic trioxide inhibits the growth of calu-6 cells via inducing a g2 arrest of the cell cycle and apoptosis accompanied with the depletion of gsh. *Cancer Lett* 2008;**270**:40–55
58. Fei F, Yu Y, Schmitt A, Rojewski MT, Chen B, Greiner J, Gotz M, Bunjes D, Schmitt M. Effects of nilotinib on regulatory t cells: the dose matters. *Mol Cancer* 2010;**9**:22
59. Jorgensen HG, Allan EK, Jordanides NE, Mountford JC, Holyoake TL. Nilotinib exerts equipotent antiproliferative effects to imatinib and does not induce apoptosis in cd34+ cml cells. *Blood* 2007;**109**:4016–9
60. Perkins C, Kim CN, Fang G, Bhalla KN. Arsenic induces apoptosis of multidrug-resistant human myeloid leukemia cells that express bcr-abl or overexpress mdr, mrp, bcl-2, or bcl-x(l). *Blood* 2000;**95**:1014–22
61. Grad JM, Bahlis NJ, Reis I, Oshiro MM, Dalton WS, Boise LH. Ascorbic acid enhances arsenic trioxide-induced cytotoxicity in multiple myeloma cells. *Blood* 2001;**98**:805–13
62. Dasmahapatra G, Lembersky D, Rahmani M, Kramer L, Friedberg J, Fisher RI, Dent P, Grant S. Bcl-2 antagonists interact synergistically with bortezomib in DLBCL cells in association with JNK activation and induction of ER stress. *Cancer Biol Ther* 2009;**8**:808–19

(Received September 13, 2012, Accepted February 11, 2013)